VOL. 12, NO. 7, APRIL 2017 ISSN 1819-6608
ARPN Journal of Engineering and Applied Sciences

www.arpnjournals.com

# RECENT PROGRESS ON THE DEVELOPMENT OF A PARTICLE METHOD FOR INCOMPRESSIBLE SINGLE- AND MULTI-PHASE FLOW COMPUTATION

K. C. Ng[1], Y. H. Hwang[2] and T. W. H. Sheu[3]
[1]Centre of Fluid Dynamics, Universiti Tenaga Nasional, Selangor, Malaysia
[2]National Kaohsiung Marine University, Kaohsiung, Taiwan
[3]National Taiwan University, Taipei, Taiwan
E-Mail: nkching@uniten.edu.my

**ABSTRACT**

The use of particle method in solving the Navier-Stokes equation is attractive from the viewpoint of avoiding the explicit discretization of the nonlinear convection term adopted in the commonly used Eulerian approach. In this paper, we shall report on the progress of our recently developed particle method in solving the Navier-Stokes equation. Starting from the conventional Moving Particle Semi-implicit (MPS) method, several numerical deficiencies have been realized and this has prompted us to venture into a new hybrid particle mesh method (Moving Particle Pressure Mesh) which involves no artificial numerical treatments to ensure numerical instability. Several incompressible single phase and multiphase flow cases are studied to validate our numerical approach. It is found that the numerical results agree considerably well with the reference solutions.

**Keywords:** computational fluid dynamics (CFD), moving particle semi-implicit (MPS), moving particle pressure mesh (MPPM), particle method.

## INTRODUCTION

The Eulerian scheme such as the Finite Volume (FV) method has gained significant popularity amongst the CFD practitioners. Due to the existence of convective terms in the transport equation (e.g. momentum equation), artificial diffusion is normally employed to ensure numerical stability of the flow computation at the expense of degrading the flow accuracy. In fact, artificial diffusion is quite dominant in the First-Order Upwind Scheme (FOUS), i.e. the default convective scheme in FLUENT. This scheme is robust; however, it tends to smear a sharp flow profile and hence it is not recommended if an accurate solution is desirable. There are a lot of higher-order convective schemes (such as QUICK and MUSCL schemes in FLUENT) available, which involves complex numerical treatment of convective term in order to enhance the flow accuracy. In spite of this, users may have difficulty in obtaining convergence particularly when the flow Reynolds number is high and unstructured grid environment is encountered [1, 2].

Realizing the above shortcomings in Eulerian schemes, this has prompted us to venture into the use of Lagrangian method as an alternative way to solve the fluid flow governing equations. Here, the convective derivative term ($u.\nabla(.)$) is combined with the local derivative term ($\partial_t(.)$) to become the total derivative ($D_t(.)$). By solving this total derivative term, one can simply move the location of a fluid particle after computing its new velocity at the new time level. This has effectively avoided the need of convective discretization as practiced in the Eulerian approach. Some common Lagrangian schemes are the Smoothed Particle Hydrodynamics (SPH) method [3] and the Moving Particle Semi-implicit (MPS) method [4, 5]. However, a lot of numerical tunings are required in order to attain numerical stability as observed in our previous works [6, 7].

Recently, we have worked on a new method to address the enormous tuning efforts (which are problematic) as practiced in our previous works of Lagrangian method. We realized that most of the Lagrangian method could not assure a divergence-free velocity field (therefore, continuity of flow field could not be satisfied). A solution has been proposed by inserting an Eulerian mesh in the flow domain to enforce flow continuity. It is important to note that this Eulerian mesh is meant for discretizing the Poisson Pressure Equation (PPE) which involves no convective derivative. This method is called the Moving Particle Pressure Mesh (MPPM) method [8], which is free from any tuning parameters.

In this paper, an overview our Lagrangian method will be given, followed by some of the test cases that we have attempted so far to demonstrate the workability of our numerical scheme.

## MOVING PARTICLE SEMI-IMPLICIT (MPS)

The mass and momentum conservation equations for an incompressible fluid flow can be written as:

$$\nabla \bullet \vec{u} = 0 \tag{1}$$

$$\frac{D\vec{u}}{Dt} = -\frac{1}{\rho}\nabla P + \nu\nabla^2\vec{u} + \vec{g} \tag{2}$$

Here, $\nu$ is the kinematic viscosity, $\rho$ is the fluid density and $\vec{g}$ is the gravitational acceleration. In MPS, the gradient and the Laplacian operatorsare discretized as:

$$\nabla\phi_i = \frac{d}{n^0}\sum_{j\neq i}\frac{\phi_j - \phi_{\min}}{|\vec{r}_j - \vec{r}_i|^2}(\vec{r}_j - \vec{r}_i)w(|\vec{r}_j - \vec{r}_i|), \quad (3)$$

$$\nabla^2\phi_i = \frac{2d}{\lambda_i n^0}\sum_{j\neq i}(\phi_j - \phi_i)w(|\vec{r}_j - \vec{r}_i|). \quad (4)$$

The details of the numerical method can be found in the earlier work (Ng *et al*., 2013a).

We have applied the above method to study a lot of interesting flow physics such as dam-break problem as shown in Figure-1, which shows the predicted locations of water particles with respect to time against those experimental data reported in [4]. The predicted free-surface locations by using the laminar model and turbulence model (CX2: a zero-equation model of [9] with 2% turbulent intensity) are quite similar and agreeable with the experimental data. Also, we have even looked into the mixing case by using an oscillating impeller [6, 7] without using the rotating frame of reference as practiced in FLUENT. Results are shown in Figure-2 and the comparison of streakline evolution is encouraging. Other test case such as the flow draining problem can be found in [11]. As mentioned above, despite the encouraging flow result, a fair amount of artificial numerical treatments are needed to ensure numerical stability. For example, the term $\phi_{\min}$ appeared in the MPS gradient model is artificially introduced to generate a repulsive force for numerical stability purpose [12]. Still, in most of the test cases we have simulated so far by using MPS, the spatial and temporal fluctuations of pressure field are quite visible (numerical noise).

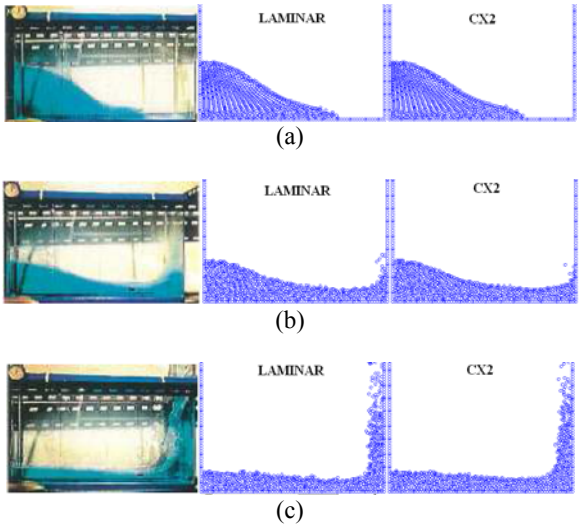


**Figure-1.** Location of water particles at (a) $t$=0.2s, (b) $t$=0.3s and (c) $t$=0.5s. CX2 model is used. The leftmost photo (experiment) is obtained from [4].

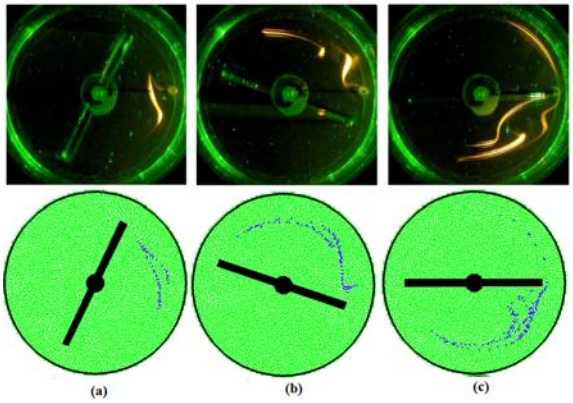


**Figure-2.** The streaklines observed by our MPS method [6] and experimental method [10] at (a) $t$=0.2$T$; (b) $t$=0.6$T$; and (c) $t$=$T$.

## MOVING PARTICLE PRESSURE MESH (MPPM)

Hwang [8] has highlighted that the above artificial numerical treatments in MPS can be avoided if the pressure is treated as an Eulerian variable. Therefore, in the works reported in [8, 13], the PPE is solved on a fixed Cartesian mesh and particle velocities are treated in Lagrangian manner as practiced in MPS. In MPPM, the PPE is written as

$$\frac{h}{\Delta t}\left(u_e^* - u_w^* + v_n^* - u_s^*\right) = \frac{1}{\rho_e^n}P_E^{n+1} + \frac{1}{\rho_w^n}P_W^{n+1} + \frac{1}{\rho_n^n}P_N^{n+1} + \frac{1}{\rho_s^n}P_S^{n+1} - \left(\frac{1}{\rho_e^n} + \frac{1}{\rho_w^n} + \frac{1}{\rho_n^n} + \frac{1}{\rho_s^n}\right)P_P^{n+1}. \quad (5)$$

The subscripts $e$, $w$, $n$, $s$ signify the east, west, north and south face, respectively, of a local background pressure mesh $P$. Here, $h$is the mesh spacing. Strict conservation of mass flux is automatically satisfied in Equation (5), whereby this favourable condition cannot be assured in most of the existing particle methods. A complete computational stencil for solving Equation (5) can be found in Figure-3. Here, the face velocity vector can be found via numerical interpolation from the particles' velocity. It is found that an accurate representation of the face velocity vector is crucial to ensure a satisfactory flow solution. In this work, we have adopted the moving least square technique for numerical interpolation of face velocities.

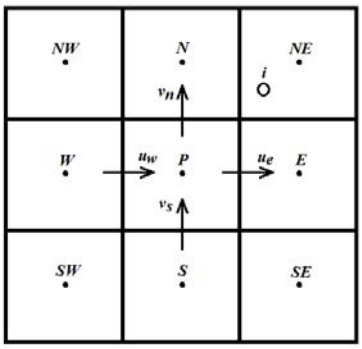


**Figure-3.** Computational stencil for PPE.

Upon obtaining the correct pressure field from Equation (5), the face velocities are then corrected as:

$$\begin{aligned}
u_e^{n+1} &= u_e^* - \frac{\Delta t}{\rho_e^n}\left(\frac{\partial P}{\partial x}\right)_e^{n+1} = u_e^* - \frac{\Delta t}{\rho_e^n}\left(\frac{P_E^{n+1}-P_P^{n+1}}{\Delta x}\right)\\
u_w^{n+1} &= u_w^* - \frac{\Delta t}{\rho_w^n}\left(\frac{\partial P}{\partial x}\right)_w^{n+1} = u_w^* - \frac{\Delta t}{\rho_w^n}\left(\frac{P_P^{n+1}-P_E^{n+1}}{\Delta x}\right)\\
v_n^{n+1} &= v_n^* - \frac{\Delta t}{\rho_n^n}\left(\frac{\partial P}{\partial y}\right)_n^{n+1} = v_n^* - \frac{\Delta t}{\rho_n^n}\left(\frac{P_N^{n+1}-P_P^{n+1}}{\Delta y}\right)\\
v_s^{n+1} &= v_s^* - \frac{\Delta t}{\rho_s^n}\left(\frac{\partial P}{\partial y}\right)_s^{n+1} = v_s^* - \frac{\Delta t}{\rho_s^n}\left(\frac{P_P^{n+1}-P_S^{n+1}}{\Delta y}\right)
\end{aligned} \quad . \tag{6}$$

The particle velocity can be corrected as well:

$$\vec{u}_i^{n+1} = \vec{u}_i^* - \frac{\Delta t}{\rho_i^n}\nabla P_i^{n+1} . \tag{7}$$

As illustrated in Figure-3, particle *i* is residing in a rectangular region enclosed by the mesh points *N*, *NE*, *P* and *E*. A bi-linear shape function can hence be defined within the rectangular region:

$$\begin{aligned}
&P_i^{n+1} = \\
&P_P^{n+1}(1-\xi_i)(1-\eta_i) + P_E^{n+1}\xi_i(1-\eta_i) + ,\\
&P_N^{n+1}(1-\xi_i)\eta_i + P_{NE}^{n+1}\xi_i\eta_i
\end{aligned} \tag{8}$$

where

$$\xi_i = (x_i - x_P)/h, \tag{9}$$

$$\eta_i = (y_i - y_P)/h. \tag{10}$$

By applying the chain rule, the pressure gradients of a particle *i*can be easily recovered as:

$$\frac{\partial P_i^{n+1}}{\partial x} = \frac{P_E^{n+1}-P_P^{n+1}}{h}(1-\eta_i) + \frac{P_{NE}^{n+1}-P_N^{n+1}}{h}\eta_i , \tag{11}$$

$$\frac{\partial P_i^{n+1}}{\partial y} = \frac{P_N^{n+1}-P_P^{n+1}}{h}(1-\xi_i) + \frac{P_{NE}^{n+1}-P_E^{n+1}}{h}\xi_i . \tag{12}$$

In contrast with the conventional MPS method, our current procedure does not require the addition of artificial repulsive force term to the pressure gradient term to ensure numerical stability.

We have tested the MPPM schemes on a few benchmark cases such as lid-driven flow and flow over a backward facing step as reported in [8]. By employing no artificial numerical treatments, we manage to achieve a fairly accurate result with the benchmark solutions. Recently, we have coupled the MPPM method with a level-set function to capture the sharp fluid interface [14]. This new method has enabled us to simulate flow of two immiscible fluids of high density ratio. Figure-4 shows the time evolution of a bubble interface. As time progresses, the bubble is rising within the surrounding heavier fluid and meanwhile changing its shape. Our numerical result compares considerably well with the reference solution [15]. We have simulated also the droplet splashing problem which involves a complex interaction of air and water as the water droplet hits the initially stagnant water pool as shown in Figure-4. Air bubbles are trapped as predicted in Figure 5-(b-d), which are agreeable with the VOF solutions from [16].

In the next example, we have considered a longer execution time for a Rayleigh-Taylor Instability (RTI) problem in order to reveal some of the interesting flow structures. As such, we have reproduced the test case recently reported in [17]. The flow domain such as that illustrated in Figure-6 is considered, by taking $W$ = 0.5m and $H$ = 4.0m. Figure-7 shows the time evolution of the fluid interface at different dimensionless time $t^* = t\sqrt{g/2W}$ obtained on the 80x640 pressure mesh, which is a finer resolution as compared to the one adopted by Shadloo *et al*. [17]. The interface predicted at $t^*$=1.8 is indeed smoother than that reported by Shadloo *et al*. [17] (c.f. their Figure-7(a)), owing to the finer resolution as well as the body-fitted arrangement of the initial particle layout. At this early time instant, the gravity drives the denser fluid into the lighter one (hence the formation of spike) and a mushroom cap starts to form at $t^*$=3.6 (Figure-7(b)). A central spike with a side tail is subsequently formed due to the continuous downward motion of the heavier fluid and its interaction with the lighter fluid as can be observed at $t^*$=5.4. Due to the domination of gravitational force over the surface tension force (=0 in the current work), one is able to notice the formation of secondary vortices (Kelvin-Helmholtz Instability) at the main spike ($y$~2.4m) owing to the substantial velocity difference between the two fluids as illustrated in Figure-7(d). Meanwhile, the side spikes ($y$~1.6m) are continuously interacting with the

neighbouring lighter fluids. The rolling and stretching motions between the fluids have subsequently turned the side spike into a very complex shape as reported in Figure-7(e).

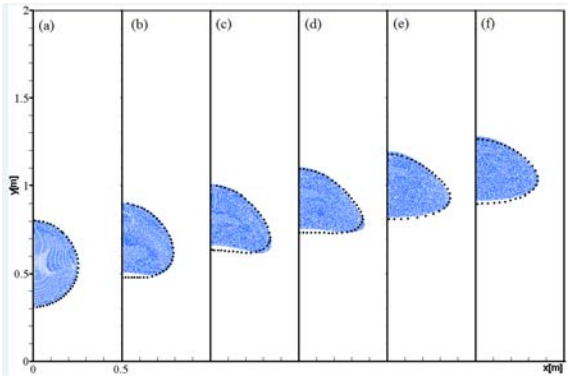


**Figure-4.** Moving particles representing the rising bubble at different time frame. Solid black dots are the Eulerian solution from Strubelj [15].

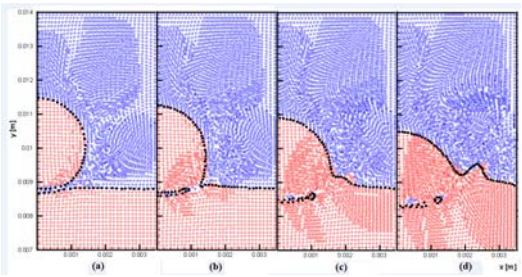

**Figure-5.** Droplet splashing at different time instants predicted by the present method and the VOF [16] method represented by solid black circles on 32x128 mesh. (a) $t$=0.0098s, (b) $t$=0.0122s, (c) $t$=0.01485s, (d) $t$=0.01781s. Red and blue particles represent water and air particles in the present method.

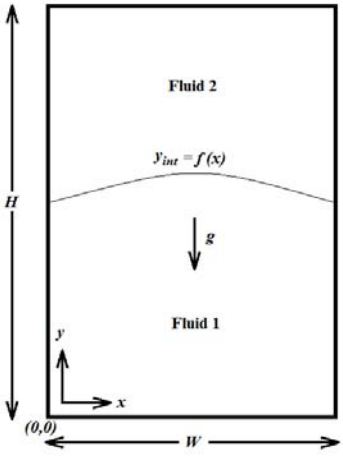


**Figure-6.** Schematic diagram of a RTI problem.

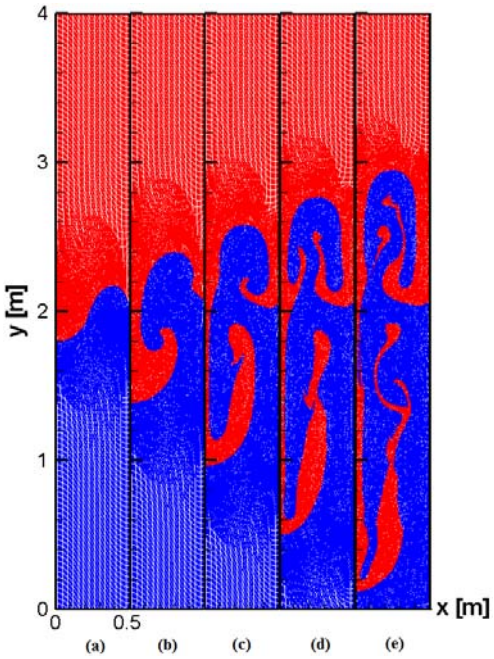


**Figure-7.** Time evolution of fluid interface at different dimensionless time $t^*$. (a) $t^*$ = 1.8; (b) $t^*$ = 3.6; (c) $t^*$=5.4; (d) $t^*$=7.2 and (e) $t^*$=9.0. Pressure mesh: 80x640. Denser fluid particles are represented by red solid circles.

## CONCLUSIONS

This paper has reported on our recent progress of development of particle method to simulate incompressible flow. The method is attractive from the viewpoint of no convective discretization is needed. The fluid particles are simply advected in space with a computed new velocity. The method has been employed to compute a series of single- and multiphase flow and good agreement has been found. Currently, we are in the midst of employing unstructured pressure mesh in order to handle a geometrically complex flow domain.

## ACKNOWLEDGEMENT

The financial supports provided by the Ministry of Education Malaysia (Project no: FRGS/2/2013/TK01/ UNITEN/02/1) and the Ministry of Science, Technology and Innovation (MOSTI) Malaysia (Project no: 06-02-03-SF0258) are greatly acknowledged and appreciated.

## REFERENCES

[1] Ng K. C., Yusoff M. Z. and Ng E.Y.K. 2007. Higher-order bounded differencing schemes for compressible and incompressible flows. International Journal for Numerical Methods in Fluids. 53(1): 57-80.

[2] Ng K. C., Ng E.Y. K., Yusoff M. Z. and Lim T.K. 2008. Applications of high-resolution schemes based on normalized variable formulation for 3D indoor

airflow simulations. International Journal for Numerical Methods in Engineering. 73(7): 948-981.

[3] Lo E.Y. M. and Shao S. D. 2002. Simulation of near-shore solitary wave mechanics by an incompressible SPH method. Applied Ocean Research. 24: 275-286.

[4] Koshizuka S., Tamako H. and Oka Y. 1995. Particle method for incompressible viscous flow with fluid fragmentation. Computational Fluid Dynamics Journal. 4: 29-46.

[5] Koshizuka S. and Oka Y. 1996. Moving-Particle Semi-Implicit method for fragmentation of compressible fluid. Nuclear Science Engineering.123: 421-434.

[6] NgK. C., Ng E.Y. K. and Lam W.H. 2013. Lagrangian simulation of steady and unsteady laminar mixing by plate impeller in a cylindrical vessel. Industrial & Engineering Chemistry Research. 52(29): 10004-10014.

[7] Ng K. C. and Ng E.Y.K. 2013. Laminar mixing performances of baffling, shaft eccentricity and unsteady mixing in a cylindrical vessel. Chemical Engineering Science. 104: 960-974.

[8] Hwang Y.H. 2011. A moving particle method with embedded pressure mesh (MPPM) for incompressible flow calculations. Numerical Heat Transfer, Part B. 60: 370-398.

[9] Ng K. C., Abdul A. M.A. and Ng E.Y.K. 2011. On the effect of turbulent intensity towards the accuracy of the zero-equation turbulence model for indoor airflow application. Building and Environment. 46(1): 82-88.

[10] KomodaY., Senda S., Takeda H., Hirata Y., and Suzuki H. 2012. 2D fluid deformation induced by a rotational reciprocating plate impeller in a cylindrical vessel. Proceedings of the14th European Conference on Mixing, Warszawa, 10–13 September 2012. pp. 211-216.

[11] Ng K. C., Ng Y. L. and Lam Y.H. 2013. Particle simulation and flow sequence on drainage of liquid particles. Computers & Mathematics with Applications. 66(8): 1437-1451.

[12] Tsuruta N., Khayyer A. and Gotoh H. 2013. A short note on dynamic stabilization of Moving Particle Semi-implicit method. Computers & Fluids. 82: 158-164.

[13] Ng K. C., Hwang Y. H. and Sheu T. W. H. 2014. On the accuracy assessment of Laplacian models in MPS. Computer Physics Communications. 185(10): 2412-2426.

[14] Ng K. C., Hwang Y. H., Sheu T. W. H. and Yu, C.H. 2015. Moving Particle Level-Set (MPLS) Method for Incompressible Multiphase Flow Computation. Computer Physics Communications.196: 317-334.

[15] Strubelj L. 2009. Numerical simulations of stratified two-phase flows with two-fluid model and interface sharpening. Ph.D. Thesis, University of Ljubljana. 125 pages.

[16] Puckett E. G., Almgren A. S., Bell J.B., Marcus D. L. and Rider W.J. 1997. A higher-order projection method for tracking fluid interfaces in variable density incompressible flows. Journal of Computational Physics. 130: 269-282.

[17] Shadloo M. S., Zainali A. and Yildiz M. 2013. Simulation of single mode Rayleigh-Taylor instability by SPH method. Computational Mechanics. 51(5): 699-715.